

ELECTRON-PHONON COUPLING ORIGIN OF THE RESISTIVITY IN $\text{YNi}_2\text{B}_2\text{C}$ SINGLE CRYSTALS

R. S. GONNELLI, A. MORELLO, G. A. UMMARINO

*INFN - Dipartimento di Fisica, Politecnico di Torino, c.so Duca degli Abruzzi, 24 -
10129 Torino, Italy*

V. A. STEPANOV

*P.N. Lebedev Physical Institute, Russian Academy of Sciences,
Leninski Pr. 53, Moscow, Russia*

G. BEHR, G. GRAW, S. V. SHULGA, S. -L. DRECHSLER

*Institut für Festkörper- und Werkstofforschung Dresden,
Postfach 270016, D-01171 Dresden, Germany*

Resistivity measurements from 4.2 K up to 300 K were made on $\text{YNi}_2\text{B}_2\text{C}$ single crystals with $T_c = 15.5$ K. The resulting $\rho(T)$ curve shows a perfect Bloch-Grüneisen (BG) behavior, with a very small residual resistivity which indicates the low impurity content and the high crystallographic quality of the samples. The value $\lambda_{\text{tr}} = 0.53$ for the transport electron-phonon coupling constant was obtained by using the high-temperature constant value of $d\rho/dT$ and the plasma frequency reported in literature. The BG expression for the phononic part of the resistivity $\rho_{\text{ph}}(T)$ was then used to fit the data in the whole temperature range, by approximating $\alpha_{\text{tr}}^2 F(\Omega)$ with the experimental phonon spectral density $G(\Omega)$ multiplied by a two-step weighting function to be determined by the fit. The resulting fitting curve perfectly agrees with the experimental points. We also solved the real-axis Eliashberg equations in both s - and d -wave symmetries under the approximation $\alpha^2 F(\Omega) \approx \alpha_{\text{tr}}^2 F(\Omega)$. We found that the value of λ_{tr} here determined in single-band approximation is quite compatible with T_c and the gap Δ experimentally observed. Finally, we calculated the normalized tunneling conductance, whose comparison with break-junction tunnel data gives indication of the possible s -wave symmetry for the order parameter in $\text{YNi}_2\text{B}_2\text{C}$.

1 Introduction

In the past seven years, a great interest has been aroused by the discovery of the family of superconducting quaternary rare-earth borocarbide intermetallic compounds $\text{RNi}_2\text{B}_2\text{C}$ ($R =$ rare earth), of which $\text{YNi}_2\text{B}_2\text{C}$ is one of the most studied non-magnetic members. In some way similarly to high- T_c cuprates, the borocarbides have a layered crystal structure, even if band-structure calculations have shown the presence of a three-dimensional electronic structure (see Ref. [1] for a short overview of selected properties). Initially, a conventional BCS description of the superconducting properties in these materials has been supported by many of the experimental and theoretical results. More recently some particular features of the electronic specific heat (as a function of temperature and magnetic field) and of the upper critical field in the non-magnetic borocarbides $\text{LuNi}_2\text{B}_2\text{C}$ and $\text{YNi}_2\text{B}_2\text{C}$ have been interpreted as signs of an unconventional pairing, possibly of d -wave type². On the other hand, Shulga *et al.* have recently explained the positive curvature of the upper critical field of $\text{YNi}_2\text{B}_2\text{C}$ as a function of the temperature near T_c , its magnitude and shape in the framework of s -wave Migdal-Eliashberg theory by

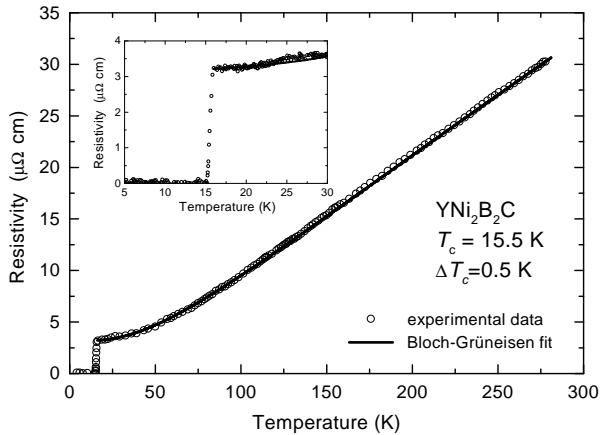


Figure 1: A few points of the typical resistivity of one of our $\text{YNi}_2\text{B}_2\text{C}$ single crystals (open circles) and the fit using the Bloch-Grüneisen model (solid line). The inset shows the low temperature part of the resistivity and the fit with all the measured points.

considering the presence of two bands, one of them being more deeply involved in the transport properties of the compound³.

In the present work we demonstrate the complete agreement of the experimental resistivity data obtained in $\text{YNi}_2\text{B}_2\text{C}$ with the predictions of the classic single-band theory for the electron-phonon (e-p) interaction (Bloch-Grüneisen theory). We obtain a value of the transport e-p coupling constant that well agrees with previous experimental and theoretical results. The transport e-p spectral function $\alpha_{\text{tr}}^2 F(\Omega)$ is also obtained by the fit of the experimental data in the whole temperature range and used for the calculation of the normalized tunneling conductance by directly solving the real-axis Eliashberg equations.

2 Experiment

High-quality $\text{YNi}_2\text{B}_2\text{C}$ single crystals were grown by using the rf - zone melting process⁴. The critical temperature of the crystals, measured by AC susceptibility and perfectly confirmed by resistivity measurements, is $T_c = 15.5$ K with $\Delta T_c(10 - 90\%) = 0.5$ K. The imaginary part of the susceptibility shows a single, very high and narrow peak at $T \approx T_c$ which confirms the purity and crystallographic quality of the samples.

We measured the resistivity of these crystals as a function of the temperature, on cooling from 300 K down to 4.2 K, by using the AC version of the standard four-probe technique. The current leads were directly soldered to the opposite sides of the samples, which have parallelepipedal shape. The voltage leads, made from very thin gold wires, were glued with a conducting paste to the surface of the crystals. We improved the sensitivity of the measurement by injecting in the crystals an AC current of typically 10 mA at 133 and detecting the voltage by the standard lock-in technique. Due to a very slow cooling-down procedure, we were able to collect

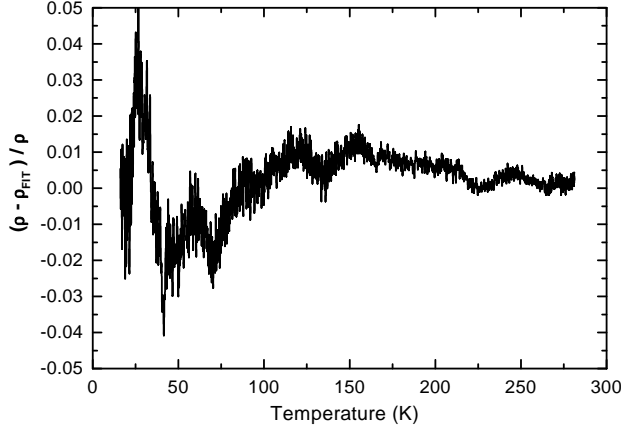


Figure 2: The relative deviations $(\rho - \rho_{\text{FIT}})/\rho$ of the experimental data from the fit.

nearly three thousand resistivity values for every curve between 4.2 and 300 K.

In Figure 1 the resistivity $\rho(T)$ of one of the $\text{YNi}_2\text{B}_2\text{C}$ crystals is shown (open circles). For clarity, only a reduced number of points is reported. In the inset of the same figure we show an enlargement of the low-temperature part of the resistivity curve that contains all the measured points at $T < 30$ K (open circles).

The resistivity of Fig. 1 shows a *perfect* Bloch-Grüneisen (BG) behavior that has already been observed in previous experiments⁵. The small residual value of the resistivity $\rho(0) = 3 \mu\Omega\cdot\text{cm}$ and its perfectly linear high-temperature part (with a slope $d\rho/dT = 0.12 \mu\Omega\cdot\text{cm}/\text{K}$) indicate the high quality and low impurity content of the samples. Quite similar results were obtained in various $\text{YNi}_2\text{B}_2\text{C}$ samples.

3 Discussion

The resistivity of a normal Fermi-liquid metal follows the well known Matthiessen's rule: $\rho(T) = \rho_0 + \rho_{\text{ph}}(T)$, where ρ_0 and $\rho_{\text{ph}}(T)$ are the residual and the phonon resistivities, respectively.

According to the BG theory, the high-temperature part of the $\rho_{\text{ph}}(T)$ shows a linear behavior given by the following expression:

$$\rho_{\text{ph}}(T) = (2\pi\varepsilon_0 k_B / \hbar\omega_p^2) \lambda_{\text{tr}} T$$

where ω_p is the plasma frequency, $\lambda_{\text{tr}} = 2 \int_0^\infty [\alpha_{\text{tr}}^2 F(\Omega) / \Omega] d\Omega$ is the transport e-p coupling constant, and $\alpha_{\text{tr}}^2 F(\Omega)$ is the transport e-p spectral function. Once known the experimental value of the plasma energy $\hbar\omega_p$ and the temperature coefficient of the linear part of the resistivity at $T > 100$ K (see Fig. 1), we can determine the transport coupling constant $\lambda_{\text{tr}} = (\hbar\omega_p^2 / 2\pi\varepsilon_0 k_B) d\rho_{\text{ph}}/dT = (\hbar\omega_p^2 / 2\pi\varepsilon_0 k_B) d\rho/dT$. The values $\omega_p = 4.25$ eV determined in Ref. [6] by reflectance and EELS measurements and $d\rho/dT = 0.12 \mu\Omega\cdot\text{cm}/\text{K}$ from Fig. 1 lead to the result $\lambda_{\text{tr}} = 0.53$.

Full information on the e-p coupling in $\text{YNi}_2\text{B}_2\text{C}$ can be obtained by fitting the resistivity of Fig. 1 in the whole temperature range. Again following the standard

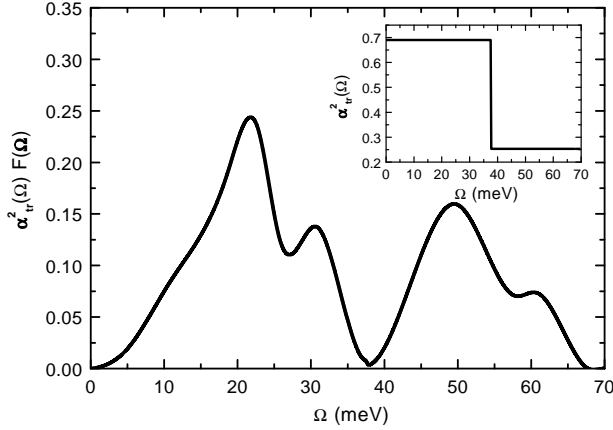


Figure 3: The electron-phonon spectral function determined from the fit of the resistivity of Fig. 1. In the inset the step-like e-p coupling function obtained from the fit is shown.

BG theory, we use the most general expression for $\rho_{\text{ph}}(T)$, given by:

$$\rho_{\text{ph}}(T) = (4\pi\varepsilon_0 k_{\text{B}} T / \hbar \omega_{\text{p}}^2) \int_0^{\Omega_{\text{max}}} [\alpha_{\text{tr}}^2 F(\Omega) / \Omega] \cdot [\hbar \Omega / 2k_{\text{B}} T \sinh(\hbar \Omega / 2k_{\text{B}} T)]^2 d\Omega.$$

Our goal is to determine the function $\alpha_{\text{tr}}^2 F(\Omega)$ from the fit. Actually, as a first approximation, for the $\alpha_{\text{tr}}^2 F(\Omega)$ we use the phonon spectral density $G(\Omega)$ obtained in inelastic neutron scattering experiments⁷ multiplied by a two-step weighting function, whose constant values for $\Omega < 37.5$ meV and $37.5 < \Omega < 70$ meV are to be determined by the fit. These energy ranges are chosen because they correspond to the two most-distinguishable structures of the $G(\Omega)$ which shows peaks at about 20 and 50 meV and a value close to zero just at 37.5 meV. We neglected in the fit the presence of high energy phonons at about 100 meV.

The results of the fit are shown as a solid line in Fig. 1. The experimental $\rho(T)$ is *perfectly* fitted by the theoretical BG curve in the whole temperature range. Fig. 2 shows the relative deviations of the experimental curve from the fit $(\rho - \rho_{\text{FIT}}) / \rho$ as function of temperature. They never exceed $\pm 5\%$.

Fig. 3 shows the spectral function $\alpha_{\text{tr}}^2 F(\Omega)$ obtained as the product of the $G(\Omega)$ by the two-step weighting function α_{tr}^2 determined from the fit. The latter function is shown in the inset of Fig. 3. Of course, the λ_{tr} calculated from the $\alpha_{\text{tr}}^2 F(\Omega)$ perfectly coincides with the value previously obtained from the linear part of $\rho(T)$.

It is well known that, to a first approximation, $\lambda_{\text{tr}} \approx \lambda$, where λ is the e-p coupling factor involved in the BCS coupling of the Cooper's pairs. In the hypothesis of an e-p coupling origin of the superconductivity in $\text{YNi}_2\text{B}_2\text{C}$ we calculate the quasiparticle density of states in this compound in both *s*- and *d*-wave symmetry by solving in direct way the real-axis Eliashberg equations for the strong e-p coupling⁸ and using as $\alpha_{\text{tr}}^2 F(\Omega)$ the function shown in Fig. 3.

Fig. 4 shows the SIN tunneling conductances in *s*- and *d*-wave symmetry calculated at 4.2 K from the density of states (solid and dash lines, respectively). From the solution of the Eliashberg equations we obtained both the correct T_c and the su-

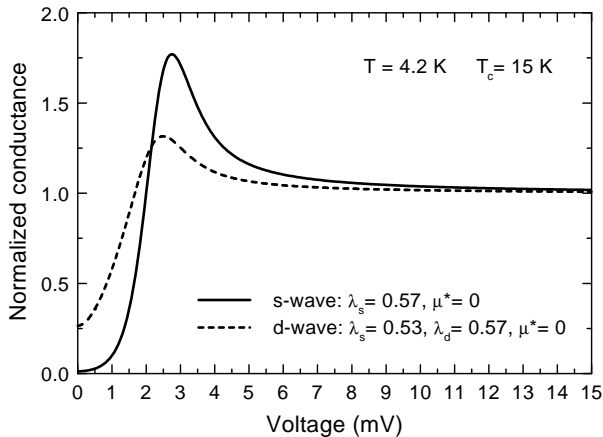


Figure 4: *s*- and *d*-wave SIN tunneling conductance of YNi₂B₂C calculated by direct solution of the Eliashberg equations using the e-p spectral function shown in Fig. 3 and the parameters shown in the legend.

perconducting gap $\Delta \approx 2$ meV observed in tunneling experiments^{9,10,11}, by using a value $\lambda = 0.57$ slightly greater than λ_{tr} . This fact is consistent with the conventional relation between λ and λ_{tr} . From the curves of Fig. 4 and the tunneling experimental data in STM configuration^{10,11} it is very difficult to determine the possible symmetry of the order parameter in YNi₂B₂C due to the appreciable broadening of the SIN data.

A more clear indication can be obtained by the comparison of the calculated SIS tunneling conductance with the break-junction experimental data present in literature. This comparison is shown in Fig. 5 where the theoretical SIS curves at 4 K determined from the solution of Eliashberg equation for pure *d*-wave (dash line), pure *s*-wave (dot line) and *s*-wave plus magnetic impurities in quasi non-unitary limit¹² (solid line) are presented together with the break-junction data of Ekino *et al*⁹ (inset). The *s*-wave curve in presence of a small amount of magnetic impurities (for details see the caption of the figure and Ref. [12]) reproduces all the main features of the experimental data including the well pronounced dip at about twice the energy of the gap. On the other hand, the *d*-wave tunneling conductance is quite different from the experimental curve. These results suggest a possible *s*-wave symmetry (or, at least, a dominant *s*-wave component) in YNi₂B₂C and give evidence for the essential role played by the electron-phonon coupling in the pairing mechanism in this compound.

4 Conclusions

We have demonstrated that the resistivity of YNi₂B₂C has a temperature dependence *perfectly* described by the standard BG theory for the e-p coupling in conventional metals. The value of λ_{tr} here determined from the resistivity is representative of an intermediate e-p coupling strength and is consistent with the value used in Ref. [3] for the discussion of the superconducting properties of YNi₂B₂C in the

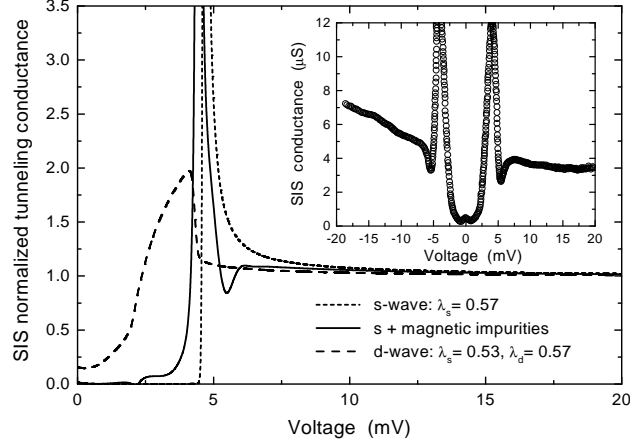


Figure 5: *s*- and *d*-wave SIS tunneling conductance of $\text{YNi}_2\text{B}_2\text{C}$ (dot and dash line, respectively) calculated by direct solution of the Eliashberg equations using the e-p spectral function shown in Fig. 3 and the parameters indicated in the legend. The solid line represents the *s*-wave SIS conductance for $\lambda_s = 0.57$ in presence of a small amount of magnetic impurities corresponding to the parameters $C_0=4$ and $\Gamma=0.8$ of the model of Ref. [12]. The inset shows the break-junction tunneling conductance at 4.4 K from Ref. [9].

framework of the isotropic single-band model. The transport e-p spectral function $\alpha_{\text{tr}}^2 F(\Omega)$ determined from the fit of the resistivity was used, to a first approximation, in the direct solution of the Eliashberg equations both in *s*- and *d*-wave symmetry. The resulting T_c and Δ are quite in agreement with the experimental data, while the comparison of the calculated SIS tunneling conductance with the break-junction data supports a conventional *s*-wave symmetry for the order parameter in $\text{YNi}_2\text{B}_2\text{C}$.

References

1. S.-L. Drechsler *et al.*, Physica C 317–318 (1999) 117.
2. G. Wang and K. Maki, Phys. Rev. B 58 (1998) 6493.
3. S.V. Shulga *et al.*, Phys. Rev. Lett. 80 (1998) 1730.
4. G. Behr *et al.*, J. Crystal Growth 198–199 (1999) 642.
5. I.R. Fisher *et al.*, Phys. Rev. B 56 (1997) 10820.
6. K. Widder *et al.*, Europhys. Lett. 30 (1995) 55.
7. F. Gompf *et al.*, Phys. Rev. B 55 (1997) 9058.
8. G.A. Ummarino and R.S. Gonnelli, Physica C 328 (1999) 189.
9. T. Ekino *et al.*, Phys. Rev. B 53 (1996) 5640.
10. R. Vaglio *et al.*, Phys. Rev. B 56 (1997) 934.
11. M. Iavarone *et al.*, J. Phys. Chem. Sol. 59 (1998) 2030.
12. C. Jiang, J.P. Carbotte, R.C. Dynes, Phys. Rev. B 47 (1993) 5325.